Carbon Dioxide Capture from Flue Gases Using a Cross-Flow Membrane Contactor and the Ionic Liquid 1-Ethyl-3-methylimidazolium Ethylsulfate

ARTICLE *in* INDUSTRIAL & ENGINEERING CHEMISTRY RESEARCH · NOVEMBER 2010

Impact Factor: 2.59 · DOI: 10.1021/ie1014266

3 AUTHORS:

Jonathan Albo
Universidad del País Vasco / Euskal Herrik…
41 PUBLICATIONS **295** CITATIONS
SEE PROFILE

Patricia Luis
University of Leuven
70 PUBLICATIONS **632** CITATIONS
SEE PROFILE

Angel Irabien
Universidad de Cantabria
348 PUBLICATIONS **3,418** CITATIONS
SEE PROFILE

Carbon Dioxide Capture from Flue Gases Using a Cross-Flow Membrane Contactor and the Ionic Liquid 1-Ethyl-3-methylimidazolium Ethylsulfate

Jonathan Albo,* Patricia Luis, and Angel Irabien

Universidad de Cantabria, Ingeniería Química y Química Inorgánica, Avda. de los Castros s/n, ES-39005 Santander, Spain

Carbon dioxide (CO_2) emissions have to be controlled and reduced in order to avoid environmental risks. Membrane processes in combination with the use of ionic liquids are recently under research and development in order to demonstrate a zero solvent emission process for CO_2 capture. In this work, the application of a cross-flow membrane contactor is studied for CO_2 absorption when the ionic liquid 1-ethyl-3-methylimidazolium ethylsulfate is used as solvent. A mathematical model considering a parallel flow configuration is applied for a cross-flow system in order to describe the mass transfer rate. At a macroscopic level, $K_{overall}a$ is calculated considering different mixing models corresponding to plug flow and continuous stirred models and a first order mass transfer rate. A microscopic model based on laminar flow has been applied, obtaining a membrane mass transfer coefficient of $k_m = 3.78 \times 10^{-6}$ m·s^{-1}, which is about five times higher than that obtained in the macroscopic model. The interfacial area, a, allows the comparison of efficiencies between cross-flow and parallel membrane contactor systems in terms of the product ($K_{overall}a$).

1. Introduction

Carbon dioxide (CO_2) is one of the major contributors to the greenhouse effect. The power and industrial sectors combined account for about 60% of the global CO_2 emissions.[1,2] CO_2 capture and storage (CCS), which involves the processes of capture, transport, and long-term storage of carbon dioxide, is a technology aimed at reducing greenhouse gas emissions from burning fossil fuels during industrial and energy-related processes. However, CO_2 capture is the bottleneck step where efforts have to be applied in order to develop technically and economically available processes.

Gas absorption processes for CO_2 removal at industrial scale are normally carried out in packed or spray towers. This technology involves many environmental and economic drawbacks, including solvent losses associated with the direct contact between the gas and liquid phases. Previous works[3−5] showed that process intensification can be performed in two steps to develop a zero solvent emission process:[3] first by the substitution of the equipment for a membrane device avoiding dragging of solvent drops[6] and second by the substitution of the absorption liquid for a solvent with lower vapor pressure (e.g., ionic liquids).[3]

Membrane contactors avoid dispersion of one phase into another, since the membrane behaves as a physical barrier. The use of this membrane-based technology supposes a relatively new concept in gas absorption processes and offers many advantages, including high surface area per unit volume.[6−13] Specifically, CO_2 absorption using hollow fiber membrane contactors is being studied in the literature.[6−9,12−15]

Two different kinds of contactors are considered: parallel and cross-flow membrane contactors, depending on the relative flow directions of the fluids. In cross-flow operation, the concentration of both fluids varies in both directions: in the direction of the flow as well as in the direction perpendicular to the flow. Thus, the theory of a cross-flow membrane contactor turns out to be rather complicated, when predicting its performance.[15]However, from an experimental point of view, this disposition seems to be better, since it offers many advantages, such as higher mass transfer coefficients and lower shell-side pressure drop when compared to the parallel flow.[16] These advantages are mainly based on the gas flow path taken in the shell-side, affecting the performance of the module in two ways. First, the extent of mass transfer varies from streamline to streamline due to the residence time distribution and channeling of the shell-side fluid. Spread in residence time and channeling effects result in lower mass transfer rates. As cross-flow contactors have reduced channeling, their performance is comparatively better. Second, the local mass transfer resistance is a function of local velocity and turbulence. In the case of cross-flow contactors, concentration boundary layer break-up occurs due to continuous splitting and remixing of the shell-side fluid, thus increasing the local turbulence level.[15]

Previous studies have reported the performance of cross-flow gas−liquid contactors considering the same flow per membrane area and equal flow per module volume, resulting in more efficiency values as compared to parallel flow modules.[17] Wickramasinghe et al.[18] used new modules with fibers evenly spaced, which yielded faster mass transfer than that obtained in commercially available modules. Also, Jansen et al.[19] used polypropylene hollow fiber membrane modules in cross-flow disposition for SO_2 absorption, obtaining a value of mass transfer one order of magnitude higher than that of conventional parallel modules. Analytical expressions have been derived in the literature to describe the mass transfer in these hollow fiber cross-flow contactors analogously to heat transfer in cross-flow shell and tube heat exchangers.[20]

In this work, the study of mass transfer modeling for CO_2 removal in a cross-flow membrane contactor (Liqui-Cel, United States) is presented when the ionic liquid 1-ethyl-3-methylimidazolium ethylsulfate is used as solvent. The applied model has been described in a previous work[4] for a hollow fiber membrane contactor in parallel disposition and countercurrent flow, using a laminar flow model in the tube side and Happel's free surface model[21] in the shellside adapted to the cross-flow geometry by means of the fiber packing density parameter. Thus, a simple mathematical model is applied for a cross-flow membrane contactor configuration at the macroscopic level, allowing comparison of

* To whom correspondence should be addressed. Telephone:+34 942 206777. Fax: +34 942 201591. E-mail: alboj@unican.es.

10.1021/ie1014266
Published on Web 09/24/2010

Table 1. Module Specifications

fiber o.d., d_0 (m)	3×10^{-4}
fiber i.d., d_i (m)	2.2×10^{-4}
fiber length, L (m)	0.015
number of fibers, n	700
effective inner membrane area, A (m^2)	0.01
contactor volume (m^3)	3.4×10^{-6}
shell side volume, V_{sh} (m^3)	2.7×10^{-6}

Table 2. Operating Conditions

	[EMIM][$EtSO_4$]
pressure at the inlet of gas line (bar gauge)	0
pressure at the inlet of liquid line (bar gauge)	0.210
pressure drop (gas line) (bar)	0
pressure drop (liquid line) (bar)	0.16
composition of feed gas stream (vol %)	
CO_2	18 ± 1
N_2	rest to balance
temperature (K)	289 ± 1
gas flow rate ($mL \cdot min^{-1}$)	2.5
liquid flow rate ($mL \cdot min^{-1}$)	20

different equipments, and at the microscopic level, where the influence of mass transfer variables can be analyzed.

2. Experimental Section

2.1. Materials and Methods. The ionic liquid 1-ethyl-3-methylimidazolium ethylsulfate ([EMIM][$EtSO_4$]), commonly named EMISE, was used as the absorption liquid due to its low viscosity at room temperature and low cost[3] in addition to its low toxicity.[22] EMISE was kindly supplied by Green Solutions (Vigo, Spain). Carbon dioxide (99.7 ± 0.01 vol %) was obtained from Air Liquide (Spain), and pure nitrogen (99.999 ± 0.001 vol %) from Air Liquide (Spain) was used to dilute the gas stream.

The hydrophobic hollow fiber contactor was supplied by Liquicel-Membrane Contactors (USA). According to the commercial specifications, the microporous hollow fiber membrane is a thin wall, opaque, polypropylene membrane with a nominal internal diameter of 220 μm. The wall thickness is 40 μm, leading to a symmetric membrane. The pore size of the fiber is 0.04 μm, and the porosity is 40% ($\varepsilon = 0.4$).

The potting and housing material are epoxy and polycarbonate, respectively. In the hollow fiber membrane contactor, the gas stream flows through the shell side, and the absorption liquid flows counter-currently through the inside of the hollow fibers. The hollow fiber contactor features are shown in Table 1. The composition of the feed gas stream (typical from combustion processes) is $18 \pm 1\%$ CO_2 and N_2 (rest to balance). The range of experimental conditions and the experimental setup are shown in Table 2 and Figure 1, respectively.

The feed gas stream was adjusted by means of a mass flow controller (Brook Instrument MFC 5850, Emerson Process Management Spain), which allows control and measurement of the flow of each gas line. Pressure gauges at the contactor inlet and outlet show the gas pressure, while a needle valve was installed in the exit gas line in order to maintain the desired pressure, if necessary. The solvent was pumped from the storage tank. Control and measurement in the liquid line was carried out with a digital gear pump (Cole Parmer Instrument Company, Hucoa-Erloss S.A, Spain), which permits control of the liquid flow. A valve was used in the outlet to prevent accidental passing of gas bubbles into the liquid. The measurement of pressure in the liquid line was similar to that in the gas line.

Pseudosteady state was obtained after about 1 h of operating time for the studied range of carbon dioxide concentration. The mass transfer flux of carbon dioxide in the gas phase has been calculated according to this equation:

$$N_{CO_2,g} = \frac{Q_g}{A}(C_{CO_2(g),in} - C_{CO_2(g),out}) \quad (1)$$

where Q_g is the gas flow rate and A is the membrane area.

The overall mass transfer coefficient, $K_{overall}$, can be experimentally evaluated from the flux through the membrane:

$$N_{CO_2,g} = K_{overall}\frac{\Delta y_{lm} P_T}{RT} \quad (2)$$

P_T is the total pressure in the gas phase, and Δy_{lm} is the logarithmic mean of the driving force based on gas phase molar fractions and taking into account the carbon dioxide concentration in the inlet ($y_{CO_2(g),in}$) and outlet ($y_{CO_2(g),out}$) of the contactor. It is assumed that the carbon dioxide concentration in the solvent is very far from the saturation in the experiments, and so the influence of the gas−liquid equilibrium has been neglected: $y^*_{in} \approx y^*_{out} \approx 0$:

$$\Delta y_{lm} = \frac{(y_{CO_2(g),in} - y^*_{in}) - (y_{CO_2(g),out} - y^*_{out})}{\ln((y_{CO_2(g),in} - y^*_{in})/(y_{CO_2(g),out} - y^*_{out}))} \quad (3)$$

The carbon dioxide flux through the membrane can also be expressed from a microscopic point of view, considering a differential portion of area in the fiber according to Figure 1:

$$N_{CO_2,g} = \frac{\partial n_A}{\partial A} = \frac{\partial n_A}{a\,\partial V} \quad (4)$$

The interfacial area, a, is defined as the ratio between the membrane area (A) and the shell side volume (V), and n_A is the number of moles per time unit that goes through the membrane. If eqs 2 and 4 are combined and integrated, the volumetric flux, $R_{CO_2,g}$, is obtained:

$$R_{CO_2,g} = (K_{overall}a)\frac{\Delta y_{lm} P_T}{RT} \quad (5)$$

This equation combines the macroscopic and microscopic levels, allowing the evaluation of the product ($K_{overall}a$), which is of interest to compare contactors with different geometries, as happens with cross-flow and parallel contactors. This work is focused on the first kind of contactors mentioned, but comparing the parameter ($K_{overall}a$), in both dispositions.

In addition, the $K_{overall}a$ product can be calculated considering different concentration profiles. By this method, it is possible to analyze the maximum and minimum values that can be achieved, which correspond to a plug flow and well mixing model at first order reaction, according to the following equations, respectively:

$$(K_{overall}a) = \frac{Q_{gas}}{V_{shellside}} \ln \frac{C_{out}}{C_{in}} \quad (6)$$

$$(K_{overall}a) = \frac{Q_{gas}}{V_{shellside}} \frac{C_{in} - C_{out}}{C_{in}} \quad (7)$$

3. Model Development

A model described in a previous work[4] for a hollow fiber contactor in parallel disposition has been adapted to the cross-flow configuration through the packing density definition, which includes the geometry.

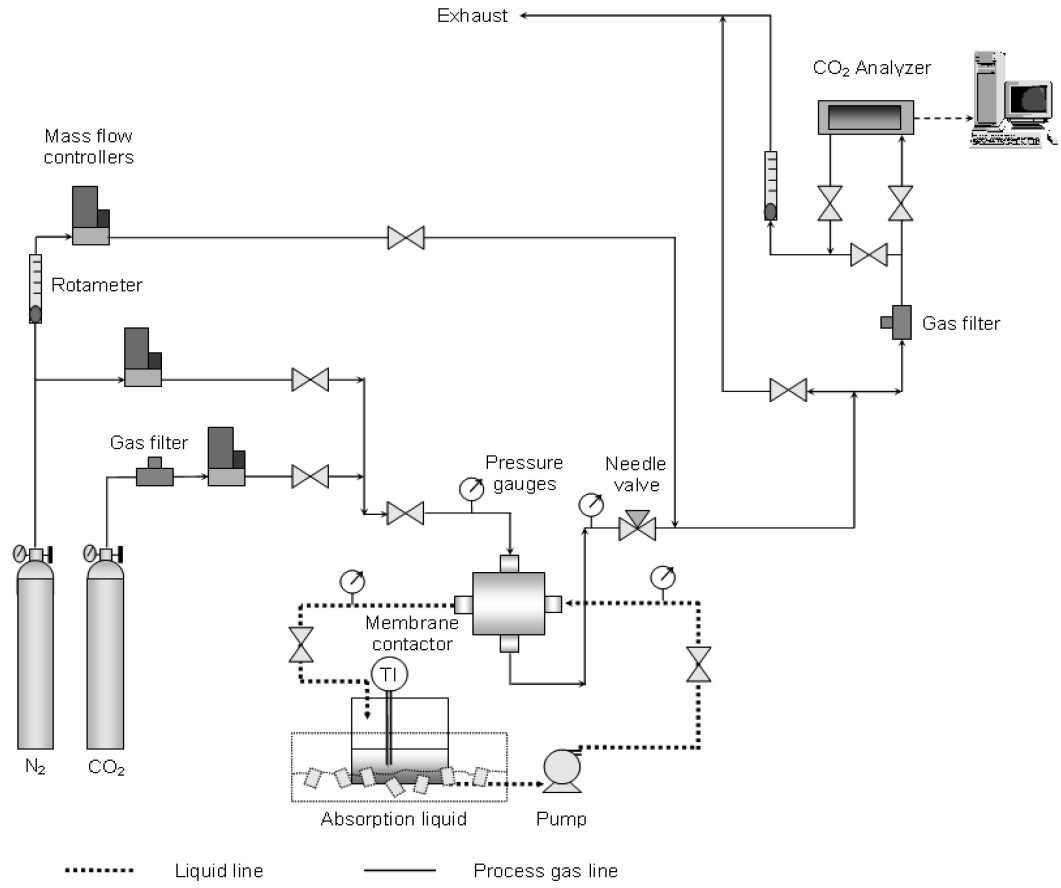

Figure 1. Experimental setup.

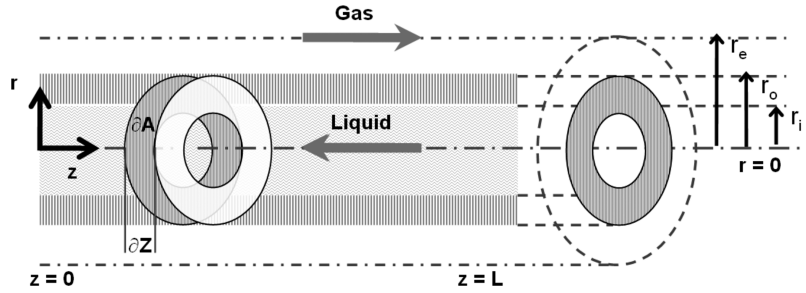

Figure 2. Axial and radial coordinates of a fiber.

In order to describe the mass transfer in the hollow fiber membrane contactor, a mass balance has been applied in the shell and tube sides. Mass transfer takes place through the membrane pores without mixing between phases. The fluid flow is described using the laminar flow model in the tube side and Happel's free surface model[21] in the shell side. This model assumes that the fibers are distributed evenly through the shell space, allowing that the obtained results with a single fiber can be generalized to the entire module.[7]

The coordinates of a fiber are shown in Figure 2. The radial position of $r = 0$ is the center of a fiber and the radial distances r_i, r_o, and r_e are the inner radius, outer radius, and Happel's free distance of the fiber. The axial distance of $z = 0$ means the inlet position of a fiber, and the axial distance of $z = L$ represents the outlet position of a fiber. The gas mixture with carbon dioxide and nitrogen is fed to the shell side at $z = 0$, and it is considered that flows in similarity as in parallel disposition to simplify the model. Liquid passed through the tube side at $z = L$. Since interfacial area has been introduced into the model, A and Z are represented in the figure. Carbon dioxide is removed from the mixture by diffusing through the membrane and, then, absorbing/reacting with the solvent. It is assumed that local equilibrium at the fluid−fluid interface takes place and mass transfer is only produced by diffusion.

3.1. Outside the Fiber. The outside of the fiber is described according to the following assumptions: (1) steady state and isothermal conditions; (2) no axial diffusion; (3) Happel's free surface model[21] to characterize the velocity profile at the shell side; (4) constant physical properties of the fluid; (5) constant shell-side pressures. Based on Happel's free surface model,[21] only a portion of the fluid surrounding the fiber is considered, which may be approximated as a circular cross section.[23]

The partial differential equation of the mass balance for cylindrical coordinates is obtained using Fick's law of diffusion, and it is given as follows:

$$u_{z,g}\frac{\partial C_{CO_2,g}}{\partial z} = D_{CO_2,g}\left[\frac{1}{r}\frac{\partial}{\partial r}\left(r\frac{\partial C_{CO_2,g}}{\partial r}\right)\right] \quad (8)$$

According to Happel's free surface model,[21] the velocity profile in the shell side may be deduced, obtaining the following equations, which have been applied by several authors.[4,12,23,24]

$$u_{z,g} = u_{max,g} f(r) = 2u_{m,g} f(r) \tag{9}$$

$$f(r) = \left[1 - \left(\frac{r_o}{r_e}\right)^2\right]\left[\frac{\left(\frac{r}{r_e}\right)^2 - \left(\frac{r_o}{r_e}\right)^2 + 2\ln\left(\frac{r_o}{r}\right)}{3 + \left(\frac{r_o}{r_e}\right)^4 - 4\left(\frac{r_o}{r_e}\right)^2 + 4\ln\left(\frac{r_o}{r_e}\right)}\right] \tag{10}$$

where r_e is the free surface radius defined as

$$r_e = \left(\frac{1}{\varphi}\right)^{0.5} r_o \tag{11}$$

and ϕ is the fiber packing density, where a cross-flow geometry is considered. It is calculated as the ratio between the volume occupied by the fibers and the total volume of the contactor.

$$\varphi = \frac{n\pi {r_o}^2 L_f}{L^2 w} = \frac{A}{V_{sh}}\left(\frac{r_o}{2}\right) \tag{12}$$

where n is the number of fibers; L_f is the fiber length; L and w are the length and width of the contactor, respectively; A is the effective membrane area; and V_{sh} is the shellside volume.

The boundary conditions are the following:

$$r = r_e,\ \frac{\partial C_{CO_2,g}}{\partial r} = 0;\ \text{(symmetry condition)} \tag{13a}$$

$$r = r_o,\ D_{CO_2,g}\frac{\partial C_{CO_2,g}}{\partial r} = K_m S(C_{CO_2,g} - C^*_{CO_2,g}) \tag{13b}$$

$$z = 0,\ C_{CO_2,g} = C_{CO_2,in} \tag{13c}$$

where $D_{CO_2,g}$ is the diffusion coefficient of carbon dioxide in the gas phase, S is a geometric factor based on the outer radius, and $C^*_{CO_2,g}$ is the concentration of carbon dioxide in the gas phase in equilibrium with the liquid phase at the membrane−liquid interface. It is assumed that Henry's law can be applied to establish a relationship between both phases. Thus, $C^*_{CO_2,g} = HC_{CO_2,l}$, where H is the Henry's law constant.

According to eq 13b, the mass transfer through the membrane is described in terms of a mass transfer coefficient (k_m) which involves the assumption of a single resistance of the membrane and a linear profile of the carbon dioxide concentration through the thickness of the membrane.

The differential mass balance in eq 8 was made dimensionless by introducing the following dimensionless variables:

$$\theta = \frac{r}{r_o},\ \bar{z} = \frac{z}{L},\ \bar{C}_{CO_2,g} = \frac{C_{CO_2,g}}{C_{CO_2,in}} \tag{14a}$$

$$Sh_m = \frac{K_m S r_o}{D_{CO_2,g}}\ \text{(Sherwood number)} \tag{14b}$$

$$Gz_{ext} = \frac{u_{m,g} {d_o}^2}{D_{CO_2,g} L}\ \text{(Graetz number in the shell side, with } d_o = 2r_o) \tag{14c}$$

The resulting dimensionless mass balance and boundary conditions are as follows:

$$\frac{Gz_{ext}}{2} f(\bar{r})\frac{\partial \bar{C}_{CO_2,g}}{\partial \bar{z}} = \frac{1}{\theta}\frac{\partial}{\partial \theta}\left(\theta \frac{\partial \bar{C}_{CO_2,g}}{\partial \theta}\right) \tag{15}$$

$$f(\bar{r}) = \left[1 - \left(\frac{r_o}{r_e}\right)^2\right]\left[\frac{\left(\frac{\bar{r}\cdot r_o}{r_e}\right)^2 - \left(\frac{r_o}{r_e}\right)^2 + 2\ln\left(\frac{1}{\bar{r}}\right)}{3 + \left(\frac{r_o}{r_e}\right)^4 - 4\left(\frac{r_o}{r_e}\right)^2 + 4\ln\left(\frac{r_o}{r_e}\right)}\right] \tag{16}$$

$$\theta = \frac{r_e}{r_o},\ \frac{\partial \bar{C}_{CO_2,g}}{\partial \theta} = 0 \tag{17a}$$

$$\theta = 1,\ \frac{\partial \bar{C}_{CO_2,g}}{\partial \theta} = Sh_m(\bar{C}_{CO_2,g} - \bar{C}_{CO_2,l}) \tag{17b}$$

$$\bar{z} = 0,\ \bar{C}_{CO_2,g} = 1 \tag{17c}$$

3.2. Inside the Fiber. The absorption liquid flows through the lumen of the fiber, and the following assumptions were utilized: (1) steady state and isothermal conditions; (2) no axial diffusion; (3) fully developed parabolic liquid velocity profile in the hollow fiber; (4) constant physical properties of the fluid; and (5) constant tube-side pressure. Considering these assumptions, the mass conservation equation inside hollow fibers is given as[25]

$$u_{z,l}\frac{\partial C_{CO_2,l}}{\partial z} = D_{CO_2,l}\left[\frac{1}{r}\frac{\partial}{\partial r}\left(r\frac{\partial C_{CO_2,l}}{\partial r}\right)\right] \tag{18}$$

When the velocity is fully developed in a laminar flow, the axial velocity can be written as

$$u_{z,l} = u_{max,l}\left[1 - \left(\frac{r}{r_i}\right)^2\right] = 2u_{m,l}\left[1 - \left(\frac{r}{r_i}\right)^2\right] \tag{19}$$

Equation 8 can be rewritten as

$$2u_{m,l}\left[1 - \left(\frac{r}{r_i}\right)^2\right]\frac{\partial C_{CO_2,l}}{\partial z} = D_{CO_2,l}\left[\frac{1}{r}\frac{\partial}{\partial r}\left(r\frac{\partial C_{CO_2,l}}{\partial r}\right)\right] \tag{20}$$

The boundary conditions are the following

$$r = 0,\ \frac{\partial C_{CO_2,l}}{\partial r} = 0\ \text{(symmetry condition)} \tag{21a}$$

$$r = r_i,\ D_{CO_2,l}\frac{\partial C_{CO_2,l}}{\partial r} = D_{CO_2,g}\frac{\partial C_{CO_2,g}}{\partial r} \tag{21b}$$

$$z = L, C_{CO_2,l} = 0 \tag{21c}$$

where $D_{CO_2,l}$ is the diffusion coefficient of carbon dioxide in the liquid phase and it is assumed that the liquid does not have

any or has only a negligible quantity of carbon dioxide at the inlet of the liquid stream ($z = L$).

The bulk average or "mixing cup" value of the carbon dioxide concentration in the liquid phase at $z = 0$ (liquid outlet) is defined as

$$C_{CO_2,z=0} = \frac{\int_0^{r_i} C_{CO_2,l} u_{z,l} 2\pi r \, dr}{\int_0^{r_i} u_{z,l} 2\pi r \, dr} = \frac{4}{r_i^2} \int_0^{r_i} C_{CO_2,l} \left[1 - \left(\frac{r}{r_i}\right)^2\right] r \, dr \tag{22}$$

The above model equations can be rewritten in the dimensionless form as

$$\frac{Gz_{int}}{2}[1 - \bar{r}^2] \frac{\partial \bar{C}_{CO_2,l}}{\partial \bar{z}} = \frac{1}{\bar{r}} \frac{\partial}{\partial \bar{r}} \left(\bar{r} \frac{\partial \bar{C}_{CO_2,l}}{\partial \bar{r}} \right) \tag{23}$$

with the boundary conditions

$$\bar{r} = 0, \frac{\partial \bar{C}_{CO_2,l}}{\partial \bar{r}} = 0 \tag{24a}$$

$$\bar{r} = 1, \frac{\partial \bar{C}_{CO_2,l}}{\partial \bar{r}} = \frac{\partial \bar{C}_{CO_2,g}}{\partial \bar{r}} \frac{D_{CO_2,g}}{D_{CO_2,l}} H \tag{24b}$$

$$\bar{z} = 1, \bar{C}_{CO_2,l} = 0 \tag{24c}$$

where the dimensionless variables are defined as

$$\bar{r} = \frac{r}{r_i}, \bar{z} = \frac{z}{L}, \bar{C}_{CO_2} = \frac{C_{CO_2}}{C_{CO_2,sat}} \tag{25a}$$

$$Gz_{int} = \frac{u_{m,l} d_i^2}{D_{CO_2,l} L} \text{ (Graetz number in the tube side, with } d_i = 2r_i) \tag{25b}$$

The dimensionless mixing cup may also be rewritten as

$$\bar{C}_{CO_2,l,\bar{z}=0} = 4 \int_0^1 \bar{C}_{CO_2,l}[1 - \bar{r}^2] \bar{r} \, d\bar{r} \tag{26}$$

The numerical solutions of eqs 14a−17c and 23−26 are obtained using the commercial software *Aspen Custom Modeler* (Aspen Technology Inc., Cambridge, MA). The discretization was carried out in the radial and axial directions, considering two dimensionless radial directions, $\bar{r}$ and θ, and one dimensionless axial direction, $\bar{z}$. The fourth-order central finite difference (CDF4) was applied for both axial and radial directions.

4. Results and Discussion

Experimental results for carbon dioxide absorption in the ionic liquid EMISE are obtained in a cross-flow polypropylene hollow fiber membrane module in order to evaluate mass transfer through the membrane. The absorption flux depends on the carbon concentration at the inlet of the contactor, as shown by eq 1. The outlet concentration of carbon dioxide, calculated as $C_{CO_2(g),out}/C_{CO_2(g),in}$ at pseudosteady-state, ranged between 0.7 and 0.8. The overall mass transfer coefficient can be calculated from eq 2 as the relationship between absorption flux and driving force in the hollow fiber module. From the experimental results shown in Table 3 and considering process efficiency at the macroscopic level, ($K_{overall}a$) can be estimated referred to the mean logarithmic (ML) profile of concentrations, plug flow (PF), and the well mixing (WM) model according to eqs 5, 6, and 7, respectively. Results are shown in Table 4.

Table 3. Experimental Results

$N_{CO_2(g)}$ ($molCO_2 \cdot s^{-1} \cdot m^{-2}$)	$C_{CO_2,in}$ (%)
$(5.17 \pm 0.48) \times 10^{-6}$	18.63 ± 0.52

Table 4. ($K_{overall}a$) at the Macroscopic Level

	ML	PF	WM
($K_{overall}a$), s^{-1}	$(2.79 \pm 0.21) \times 10^{-3}$	$(2.79 \pm 0.21) \times 10^{-3}$	$(2.44 \pm 0.21) \times 10^{-3}$

Table 5. Model Parameters

$D_{CO_2,g}$, $m^2 \cdot s^{-1}$	1.468×10^{-5}
$D_{CO_2,EMISE}$, $m^2 \cdot s^{-1}$	3.020×10^{-10}
Gz_{int}	133.89
Gz_{ext}	3.67×10^{-4}
a, m^{-1}	3703.7
r_o, m	1.5×10^{-4}
r_e, m	2.85×10^{-4}
Ø	0.278
H	0.122

Table 6. ($K_{overall}a$) in Parallel (PFL) and Cross-flow (CFL) Dispositions

	PFL	CFL
a, m^{-1}	7200	3703.7
($K_{overall}a$), s^{-1}	$(2.66 \pm 0.12) \times 10^{-3}$	$(2.79 \pm 0.21) \times 10^{-3}$

It can be seen from the results how mass transfer in the gas-phase laminar regime can be explained by a plug flow model in the studied system, which is an interesting approach for a macroscopic level. In addition, it is important to consider that when interfacial area, a, is included, both the effective area and gas volume occupied in the contactor are taken into account, making possible the comparison of different equipment in terms of separation efficiency.

The microscopic study level has also been applied to establish the possibility of using the previous studied model[4] in a cross-flow configuration. By applying a simple mathematical model for a hollow fiber membrane contactor in parallel disposition and countercurrent flow, using a laminar flow model in the tube side and the Happel's free surface model in the shellside, a membrane mass transfer coefficient, k_m, can be obtained. Table 5 shows some parameters included in the model, and the studied experimental conditions expressed by the Gz numbers in the lumen and shell sides. The Henry's law constant (H) is an estimated value taken from studies focused on CO_2 absorption using 1-ethyl-3methylimidazolium-based ionic liquids.[26,27]

From eq 14b, the membrane mass transfer coefficient is estimated with the laminar flow model, resulting in a value of $k_m = 3.78 \times 10^{-6}$ $m \cdot s^{-1}$. This result is about five times higher than the macroscopic parameter, where a mass transfer coefficient of $K_{overall} = 0.74 \times 10^{-6}$ $m \cdot s^{-1}$ is achieved, according to the results shown in Tables 3 and 4.

In order to compare equipments in terms of the separations efficiency, the parameter ($K_{overall}a$) is evaluated in cross-flow and parallel membrane contactors in Table 6, when the ionic liquid EMISE is used as solvent. The mass transfer coefficient in the parallel disposition has been obtained in a previous work.[28]

A similar value of the product ($K_{overall}a$) has been obtained considering the effective area and volume of each module.

5. Conclusion

Mass transfer modeling for CO_2 removal in a polypropylene cross-flow membrane contactor when the ionic liquid 1-ethyl-

3-methylimidazolium ethylsulfate is used as the absorption liquid has been studied at macroscopic and microscopic scales. It is observed that there are not any differences between the results considering logarithmic mean concentration profiles through the contactor or a plug flow profile, because the mass transfer parameter is nearly the same.

Mass transfer has been described microscopically by means of the application of a laminar flow model and a Happels surface model. From this model, the membrane mass transfer coefficient takes a value of $k_m = 3.78 \times 10^{-6}$ m·s^{-1}, which is about five times higher than that obtained in the macroscopic study. This means that the influence of the laminar flow is included in the mass-transfer parameter.

The comparison between contactors with different flow configurations showed a similar value of the product ($K_{overall}a$), which means that the cross-flow contactors do not show any difference with parallel contactors.

Acknowledgment

This research has been funded by the Spanish Ministry of Science and Technology (Project CTM2006-00317 and Project EUI2008-03857).

Nomenclature

a = interfacial area, m^{-1}
A = membrane area, m^2
$\bar{C}_{CO_2}$ = dimensionless carbon dioxide concentration
C_{CO_2} = carbon dioxide concentration, mol·m^{-3}
$C^*_{CO_2}$ = carbon dioxide concentration at the membrane−liquid interface, mol·m^{-3}
$D_{CO_2,g}$ = gas diffusion coefficient, m^2·s^{-1}
$D_{CO_2,EMISE}$ = EMISE diffusion coefficient, m^2·s^{-1}
d_i = inside diameter of the hollow fiber, m
d_o = outside diameter of the hollow fiber, m
e = contactor width, m
Gz_{ext} = Graetz number referred to the shell side ($Gz_{ext} = u_{m,g}d_o^2D_{CO_2,g}^{-1}L^{-1}$)
Gz_{int} = Graetz number referred to the tube side ($Gz_{int} = u_{m,l}d_i^2D_{CO_2,l}^{-1}L^{-1}$)
H = Henry's law constant: the molar concentration in the gas divided by that in the liquid
K_m = mass transfer coefficient of the membrane, m·s^{-1}
$K_{overall}$ = overall mass transfer coefficient, m·s^{-1}
L = contactor length, m
L_f = fiber length, m
$N_{CO_2,g}$ = flux through the membrane, mol CO_2·s^{-1}·m^{-2}
n = number of fibers
P_T = total pressure, atm
Q_g = gas flow, m^3·s^{-1}
r = radial coordinate position, m
r_e = free surface radius according to Happel's model, m
r_i = inner radius of the fiber, m
r_o = outer radius of the fiber, m
S = geometric factor, $S = (r_o - r_i)/(r_o \ln(r_o/r_i))$
Sh_m = Sherwood number ($Sh_m = K_mSr_oD_{CO_2}^{-1}$)
u_z = velocity, m·s^{-1}
u_{max} = maximum velocity, m·s^{-1}
u_m = average velocity, m·s^{-1}
V_{sh} = shellside volume, m^3
w = contactor width, m
z = axial coordinate position, m
$\bar{z}$ = dimensionless axial coordinate position

Subscripts

g = gas
l = liquid
in = inlet of the contactor
out = outlet of the contactor

Greek Letters

Δy_{lm} = logarithmic mean of the driving force
ϕ = packing density of the module
θ = dimensionless radial coordinate position

Literature Cited

(1) Moulijn, J. A.; Stankiewicz, A.; Grievink, J.; Górak, A. Process intensification and process systems engineering: a friendly symbiosis. *Comput. Chem. Eng.* **2008**, *32* (1−2), 3–11.

(2) Stankiewicz, A.; Van Gerven, T. Structure, Energy, Synergy, Time—The fundamentals of Process Intensification. *Ind. Eng. Chem. Res.* **2009**, *48*, 2465–2474.

(3) Luis, P.; Garea, A.; Irabien, J. Zero solvent emission process for sulfur dioxide recovery using a membrane contactor and ionic liquids. *J. Membr. Sci.* **2009**, *330*, 80–89.

(4) Luis, P.; Garea, A.; Irabien, A. Modelling of a hollow fibre ceramic contactor for SO_2 absorption. *Sep. Purif. Technol.* **2010**, *72* (2), 174–179.

(5) Luis, P.; Garea, A.; Irabien, A. Sulfur Dioxide Non-dispersive absorption in *N*,*N*-dimethylaniline using ceramic membrane contactor. *J. Chem. Technol. Biotechnol. B* **2008**, *83*, 1570–1577.

(6) Simons, K.; Nijmeijer, K.; Wessling, M. Gas-liquid membrane contactors for CO_2 removal. *J. Membr. Sci.* **2009**, *340* (1−2), 214–220.

(7) Gabelman, A.; Hwang, S. T. Hollow fiber membrane contactors. *J. Membr. Sci.* **1999**, *159* (1−2), 61–106.

(8) De Montigny, D.; Tontiwachwuthikul, P.; Chakma, A. Comparing the absorption performance of packed columns and membrane contactors. *Ind. Eng. Chem. Res.* **2005**, *44*, 5726–5732.

(9) Drioli, E.; Curcio, E. Membrane engineering for process intensification: a perspective. *J. Chem. Technol. Biotechnol. B* **2007**, *82*, 223–227.

(10) Drioli, E.; Curcio, E. Membrane distillation and related operations—A review. *Sep. Purif. Rev. B* **2005**, *34* (1), 35–86.

(11) Drioli, E.; Curcio, E.; Di Profio, G. State of the art and recent progress in membrane contactors. *Chem. Eng. Res. Des.* **2005**, *83* (A3), 223–233.

(12) Karoor, S.; Sirkar, K. Gas absorption studies in microporous hollow fibre membrane modules. *Ind. Eng. Chem. Res.* **1993**, *32*, 674–684.

(13) Kreulen, H.; Smolders, C. A.; Versteeg, G. F.; Swaaij, W. P. M. Microporous hollow fibre membrane modules as gas-liquid. Part 1. Physical mass transfer in highly viscous liquids. *J. Membr. Sci.* **1993**, *78*, 197–216.

(14) Li, J. L.; Chen, B. H. Review of CO_2 absorption using chemical solvents in hollow fiber membrane contactors. *Sep. Purif. Technol.* **2005**, *41* (2), 109–122.

(15) Bhaumik, D.; Majumdar, S.; Sirkar, K. K. Absorption of CO_2 in a transverse flow hollow fiber membrane module having a few wraps of the fiber mat. *J. Membr. Sci.* **1998**, *138* (1), 77–82.

(16) Dindore, V. Y.; Brilman, D. W. F.; Versteeg, G. F. Modelling of cross-flow membrane contactors: Physical mass transfer processes. *J. Membr. Sci.* **2005**, *251* (1−2), 209–222.

(17) Wickramansinghe, S. R.; Semmens, M. J.; Cussler, E. L. Mass transfer in various hollow fiber geometries. *J. Membr. Sci.* **1992**, *69*, 235–250.

(18) Wickramansinghe, S. R.; Semmens, M. J.; Cussler, E. L. Hollow fiber modules made with hollow fiber fabric. *J. Membr. Sci.* **1993**, *84*, 1–14.

(19) Jansen, R.; Klaasen, R.; Feron, P. H. M.; Hanemaaijer, J. H.; Ter Meulen, B. P. Membrane gas absorption processes in environmental applications. In Crespo, J. G., Boddeker, K. W., Eds.; *Membrane Processes in Separation and Purification*; Kluwer Academic Publishers: Dordrecht, 1994; pp 343−356.

(20) Dindore, V. Y.; Versteeg, G. F. Gas-liquid mass transfer in a cross-flow hollow fibre module: Analytical model and experimental validation. *Int. J. Heat Mass Transfer* **2005**, *48*, 3352–3362.

(21) Happel, J. Viscous flow relative to arrays of cylinders. *AIChE J.* **1995**, *5*, 174–177.

(22) Luis, P.; Ortiz, I.; Aldaco, R.; Irabien, A. A novel group contribution method in the development of a QSAR for predicting the

toxicity (Vibrio fischeri EC_{50}) of ionic liquids. *Ecotox. Environ. Saf.* **2007**, *67*, 423–429.

(23) Al- Marzouqi, M. H.; El- Naas, M. H.; Marzouk, S. A. M.; Al-Zarooni, M. A.; Abdullatif, N.; Faiz, R. Modeling of CO_2 absorption in membrane contactors. *Sep. Purif. Technol.* **2008**, *59*, 286–293.

(24) Zheng, J. M.; Xu, Y. Y.; Xu, Z. K. Shell side mass transfer characteristics in a parallel flow hollow fiber membrane module. *Sep. Purif. Technol.* **2003**, *38*, 1247–1267.

(25) Bird, R. B.; Stewart, W. E.; Lightfoot, E. N. *Transport Phenomena*, 2nd ed.; John Wiley & Sons, Inc.: New York, 2002.

(26) Finotello, A.; Bara, J. E.; Camper, D.; Noble, R. D. Room-Temperature Ionic Liquids: Temperature Dependence of Gas Solubility Selectivity. *Ind. Eng. Chem. Res.* **2008**, *47*, 3453–3459.

(27) Yokozeki, A.; Shiflett, M. B.; Junk, C. P.; Grieco, L. M.; Foo, T. Physical and Chemical Absorptions of Carbon Dioxide in Room-Temperature Ionic Liquids. *J. Phys. Chem. B* **2008**, *112*, 16654–16663.

(28) Albo, J.; Luis, P.; Irabien, A. Absorption of coal combustion flue gases in ionic liquids using different membrane contactors. Desalination, submitted.

Received for review July 5, 2010
Revised manuscript received August 15, 2010
Accepted August 25, 2010

IE1014266